Supporting Information

Programmably Engineered Stochastic RNA Nanowalker for Ultrasensitive miRNA Detection

Dan Zhu,[a,b] Dongxia Zhao,[a] Yang Hu,[a] Tianhui Wei,[a] Tong Su,[a] Shao Su,[a] Jie Chao,[a] and Lianhui Wang[a,*]

[a]*State Key Laboratory of Organic Electronics and Information Displays & Jiangsu Key Laboratory for Biosensors, Institute of Advanced Materials (IAM), Nanjing University of Posts and Telecommunications, 9 Wenyuan Road, Nanjing 210023, China*

[b]*State Key Laboratory of Transducer Technology, Shanghai Institute of Microsystem and Information Technology, Chinese Academy of Sciences, Shanghai 200050, China*

[*]Corresponding authors

E-mail addresses:

iamlhwang@njupt.edu.cn

Table of contents:

Experimental Section

Chemicals and Materials.

Disodium hydrogen phosphate (Na_2HPO_4), sodium dihydrogen phosphate dihydrate ($NaH_2PO_4 \cdot 2H_2O$), sodium chloride (NaCl), magnesium chloride hexahydrate ($MgCl_2 \cdot 6H_2O$,≥98.0%), trisaminomethane (Tris), tetrachloroauric acid ($HAuCl_4 \cdot 4H_2O$, 99.9%), and sodium citrate were purchased from Sinopharm Chemical Reagent Co., Ltd (Shanghai, China). All chemicals were used without further purification. All solutions were prepared with Milli-Q water from a Milli-pore system. All oligonucleotides were synthesized and purified by TaKaRa Inc. (Dalian, China), and the sequences were shown in Table S1. Duplex-specific nuclease (DSN) was purchased from Evrogen Joint Stock Company (Moscow, Russia). RNase inhibitor, diethyl pyrocarbonate (DEPC), and 6-mercapto-1-hexanol (MCH) were purchased from Sigma-Aldrich. $HAuCl_4$ ($HAuCl_4 \cdot 4H_2O$, 99.9%) was purchased from China National Pharmaceutical Group Corporation.

Apparatus.

The UV-Vis absorption spectra were recorded on a UV-Vis spectrophotometer (UV-3600, Shimadzu, Japan). The diameter of AuNPs was characterized by transmission electron microscopy (TEM, Hitachi, Tokyo, Japan, HT-7700 with an accelerating voltage of 100kV). Fluorescence spectra were collected by a fluorescence spectrometer (F-900, Edinburgh Instruments Ltd, British). Hydrodynamic diameters were characterized by Dynamic Light Scattering (DLS) (Zetasizer, Malvern Instruments). All pH measurements were performed with a digital pH-meter (FE20, MettlerToledo, Shanghai, China).

Preparation of 13 nm AuNPs and polyA-SNA

13 nm AuNPs were synthesized using the standard citrate reduction method. Briefly, 3.5 mL of 1% (w/w) trisodium citrate, 0.5 mL 2% $HAuCl_4$ was rapidly added to 99.5 mL of boiling water with vigorous stirring at 120 °C. The reaction solution was maintained at its boiling point for 30 min. After cooling to room temperature with continuous stirring, the resulting colloidal suspension was stored in a brown glass container at 4 °C until use.

The fluorophore-labeled polyA-SNA were prepared by salt-aging methods. PolyA-tailed DNA or thiolated DNA was mixed with AuNPs at a molar ratio of 200:1 and gently shaken overnight at 25 °C. Subsequently, 1 M sodium phosphate buffer (1 M NaCl,100 mM PB, pH 7.4) was added five times at intervals of 20-30 minutes to reach a final concentration of 0.1 M (0.1 M NaCl, 10 mM PB, pH 7.4). The DNA-AuNP conjugates were incubated for an additional 40 hours with gentle shaking. The prepared polyA-SNA were then washed three times with 0.1 M PBS and stored at 4 °C for further use. For the preparation of polyA-SNA with different densities of DNA tracks, DNA probes with various length of polyA tails (A5-P21-F, A10-P21-F, A20-P21-F, A30-P21-F) were added into an AuNPs solution simultaneously (DNA: AuNPs = 200:1), respectively. The solution was then processed using the same steps as described above.

Quantitation of DNA Loading on AuNPs.

Firstly, the polyA-SNA labeled with fluorophores were prepared using the salt-aging protocol. The absorbance values of DNA-AuNPs were measured by UV-visible spectroscopy. The concentration of nanoparticles was calculated via Beer's law ($A = \varepsilon bc$), where $\varepsilon_{(13\ nm\ AuNP)} = 2.70\times10^8\ L\cdot mol^{-1}cm^{-1}$. To determine the concentration of DNA, MCH was added to displace DNA from the surface with a final concentration of 10 mM. After being incubated for 18 hours at 37 °C, the released fluorophore labeled DNA was collected through centrifugation and measured by a fluorescence spectrometer. The excitation and emission wavelengths for FAM were 494 nm and 520 nm, respectively. The fluorescence was then converted to molar concentrations of probes by comparing it to standard linear calibration curves obtained by measuring known concentrations of fluorescent DNA. The number of DNA per SNA was calculated by dividing the concentration of fluorescent oligonucleotides by the concentration of AuNPs. All experiments were repeated three times to obtain error bars.

miRNA Detection in Solution.

For the detection of miRNA, a certain amount of miRNA was added to 8 nM polyA-SNA. The mixture was then incubated in 10 μL of 1×DSN buffer (50 mM Tris-HCl, pH 8.0, 5 mM $MgCl_2$, 50 mM NaCl, 0.5 U/μL RNase inhibitor) for 30 minutes at room temperature for hybridization. Then, DSN was added to the reaction solution to reach a

final concentration of 0.08 U/μL, followed by incubation at 55 °C for 90 minutes. The fluorescence was detected by diluting the solution to 50 μL with 1×DSN buffer. FAM, ROX, and Cy5 were excited at 494 nm, 580 nm and 630 nm, respectively. All experiments were repeated at least three times.

miRNA Analysis in Serum Sample.

For the detection of miRNAs in serum samples, 100 μL of human serum m (obtained from Nanjing Drum Tower Hospital) was diluted with 900 μL of 1 × DSN buffer. 1 nM of miRNA-21, 1 nM of miRNA-486, or 1 nM of miRNA-155 were added to 8 nM of specific polyA-SNA and allowed to incubate in 10 μL of diluted human serum (10%) for 30 minutes at room temperature for hybridization, respectively. Then, DSN was added to the reaction solution to reach a final concentration of 0.08 U/μL and incubated at 55 °C for 90 minutes. Fluorescence detection was performed as described in the miRNA detection in solutions section. All experiments were repeated at least three times.

Table S1. Oligonucleotide sequences used in this study.

Oligonucleotide	Sequence(5'to3')
A5-P21-F	FAM-TCAAC ATCAG TCTGA TAAGC TATTT TT AAAAA
A10-P21-F	FAM-TCAAC ATCAG TCTGA TAAGC TATTT TT AAAAA AAAAA
A15-P21-F	FAM-TCAAC ATCAG TCTGA TAAGC TATTT TT AAAAA AAAAA AAAAA
A20-P21-F	FAM-TCAAC ATCAG TCTGA TAAGC TATTT TT AAAAA AAAAA AAAAA AAAAA
A30-P21-F	FAM-TCAAC ATCAG TCTGA TAAGC TATTT TT AAAAA AAAAA AAAAA AAAAA AAAAA AAAAA
SH-P21-F	FAM-TCAAC ATCAG TCTGA TAAGC TATTT TT-SH
A20-P486-F	ROX-CTCGG GGCAG CTCAG TACAG GATTT TT AAAAA AAAAA AAA AA AAAAA
A20-P155-F	Cy5-ACCCC TATCA CGATT AGCAT TAATT TTT AAAAA AAAAA AAAAA AAAAA
miRNA-21	UAGCU UAUCA GACUG AUGUU GA
miRNA-486	GAGCC CCGUC GAGGU CAUGU CCU
miRNA-155	UUAAU GCUAA UCGUG AUAGG GGU
miRNA-200b	UAAUA CUGCC UGGUA AUGAU GA
miRNA-21-SM	UAGCU UAUCA GGCUG AUGUU GA

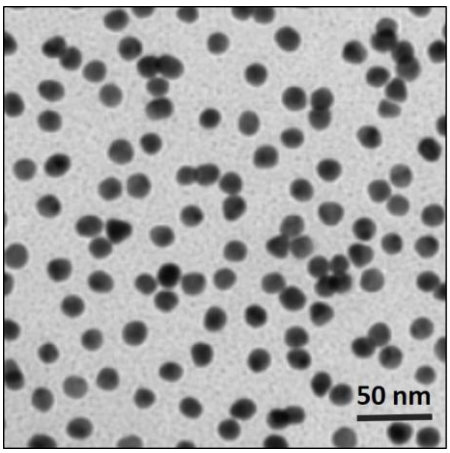

Fig. S1 The transmission electron microscope (TEM) images of bare AuNPs.

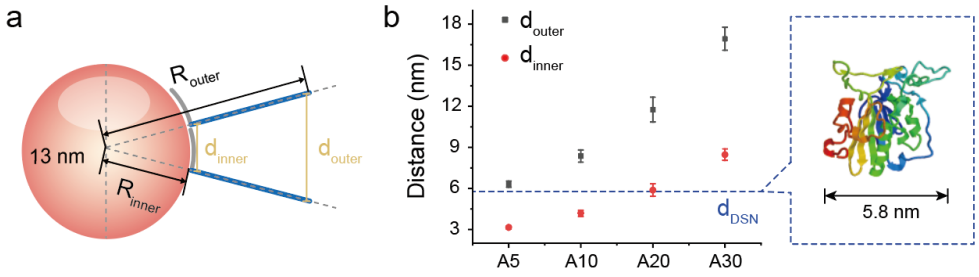

Fig. S2 (a) Estimation of the interval of DNA tracks on SNA. The distance was estimated using a model with uniformly distributed points. The accessible distances for the binding sites were calculated as $d = R * arccos\left(1 - \frac{8}{n}\right)$, Where n is the amount of experimentally obtained attached polyA strands. The distances for the outer binding sites (d_{outer}) and inner binding sites (d_{inner}) were calculated by $d_{outer} = R_{outer} * arccos\left(1 - \frac{8}{n}\right)$ and $d_{inner} = R_{inner} * arccos\left(1 - \frac{8}{n}\right)$. (b) Calculated d_{outer} (black points) and d_{inner} (red points) with different length of polyA. The inset DSN structure was simulated based on the sequence in GenBank (GenBank: AF520591.1) created using PyMol software.

We first calculated the outer and inner intervals of DNA tracks on AuNPs based on the measured densities and curvature of 13 nm AuNPs according to the reported work (Fig. S2). [1] The outer intervals (d_{outer}) are defined as the distance between the outermost DNA of the SNA, while the inner intervals (d_{inner}) refer to the distance between the DNA located on the surface of the AuNP. Furthermore, we used the PyMol software to simulate the size of the DSN enzyme through the sequence of the DSN enzyme (GenBank: AF520591.1) and found that the size of the DSN enzyme is about 5.8 nm.[2] For the RNA walker to continue moving, it is necessary for DSN to hydrolyze both the outer and inner sections of the DNA tracker so that miRNA binding and DSN hydrolysis can occur. It can be observed that A20 provides a suitable reaction space for miRNA binding and DSN hydrolysis (d_{outer} = 11.8 nm, d_{inner} = 5.9 nm). In comparison, A5 and A10 offer smaller spacing, resulting in greater steric hindrance. A30, on the other hand, has a larger spacing but lower assembly quantity, leading to a lower reaction signal. Therefore, A20 is able to create the appropriate spatial distance for DNA tracks on AuNPs surface, thereby facilitating miRNA binding and DSN hydrolysis.

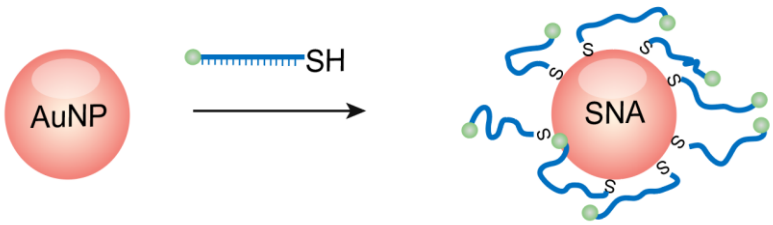

Fig. S3 Schematic illustration of the assembly of thiolated SNA by attaching sulfhydryl-modified SH-P21-F onto AuNPs.

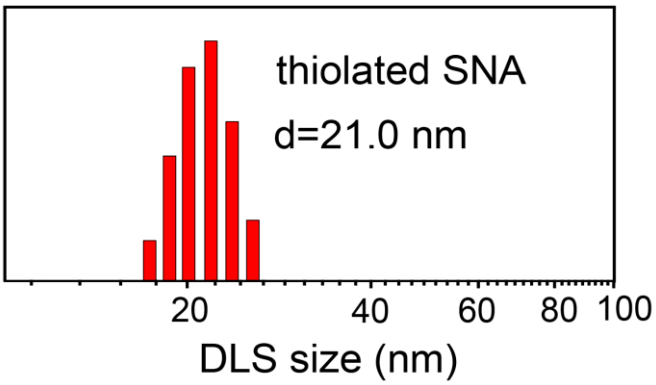

Fig. S4 Dynamic light scattering (DLS) results of thiolated SNA.

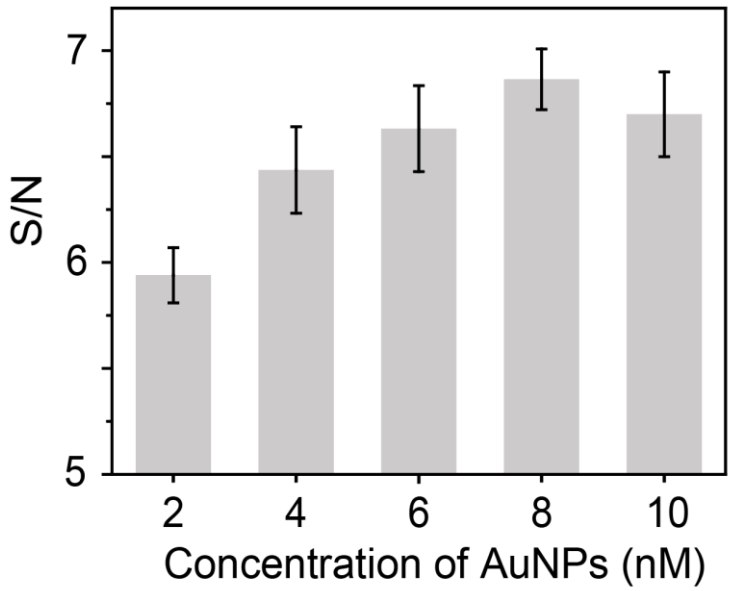

Fig. S5 The impact of concentrations of AuNPs on the polyA20-SNA powered by DSN. The experiments were performed at 42 °C after 90-min incubation with 100 nM miRNA-21 and 0.08 U/μL DSN.

A higher concentration of AuNPs could lead to the quenching of fluorescence signals, whereas a lower concentration of AuNPs might decrease the overall number of fluorescent DNA tracks. Having found that 8 nM AuNPs yielded the optimal S/N, we chose to maintain this concentration of SNA for further analyses.

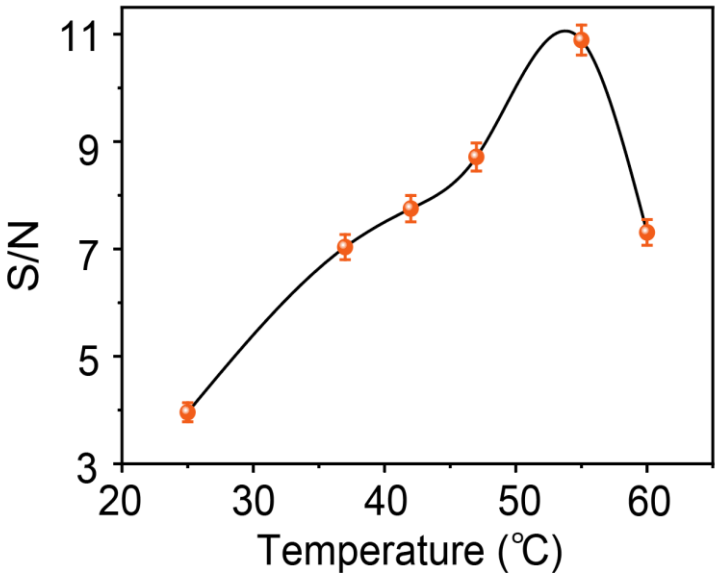

Fig. S6 The influence of temperature on the polyA20-SNA powered by DSN. The experiments were performed in 8 nM polyA20-SNA after 90-min incubation with 100 nM miRNA-21 and 0.08 U/μL DSN.

As the stochastic RNA nanowalker relied on DSN for power, the reaction temperature was then assessed in the range of 25-60 °C because DSN operates best at higher temperatures. The maximum fluorescence enhancement of the system was observed at 55 °C. Therefore, 55 °C was chosen as the optimized incubation temperature for the study.

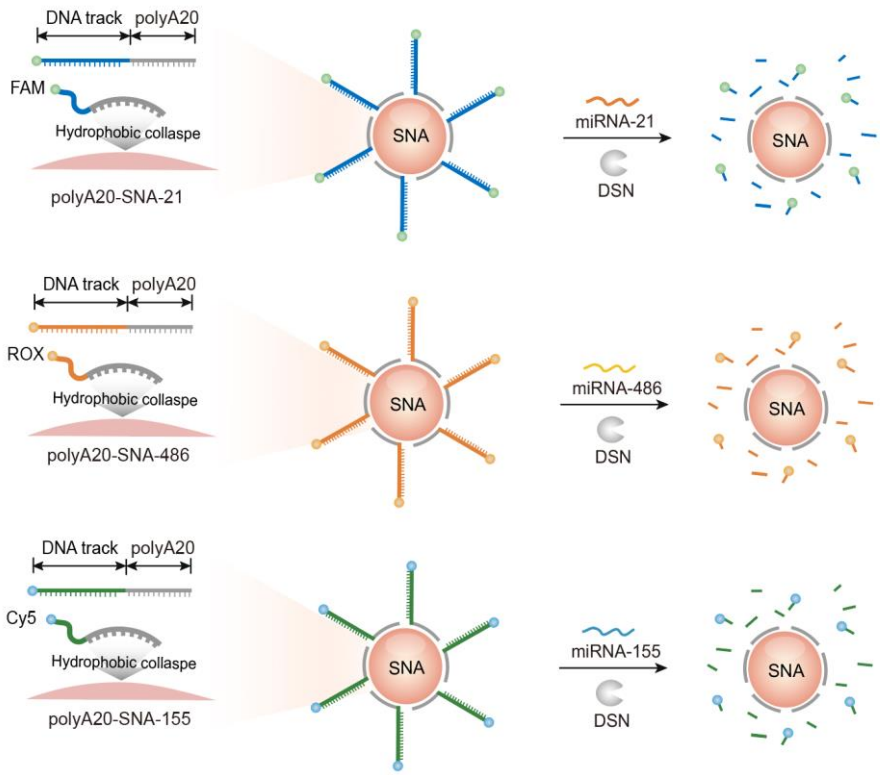

Fig. S7 Schematic illustration of the assembly and the detection process of polyA20-SNA specific for miRNA-21, miRNA-486 and miRNA-155.

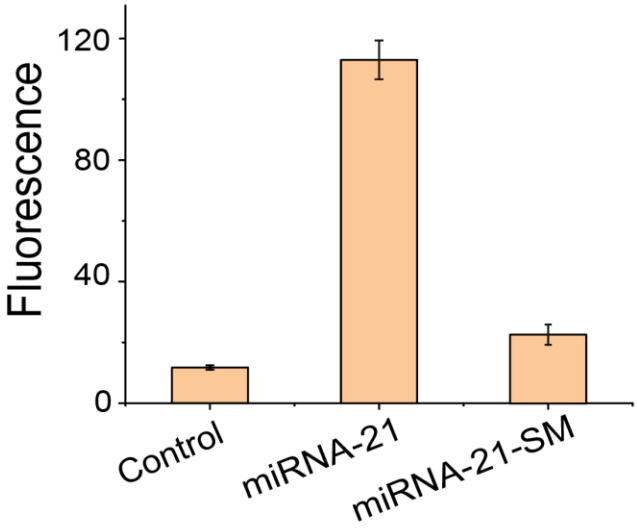

Fig. S8 The fluorescence of 8 nM polyA20-SNA (specific for miRNA-21) in the absence (control) and presence of target miRNA-21 and miRNA-21-SM.

To assess the specificity of polyA20-SNA in distinguishing single-base mismatched targets, miRNA target with a single-base mismatch (miRNA-21-SM) was chosen as the target for detection. The signal for the target miRNA-21 is shown to be around 4.2 times greater than that for miRNA-21-SM, indicating the probe's ability to detect base mismatches.

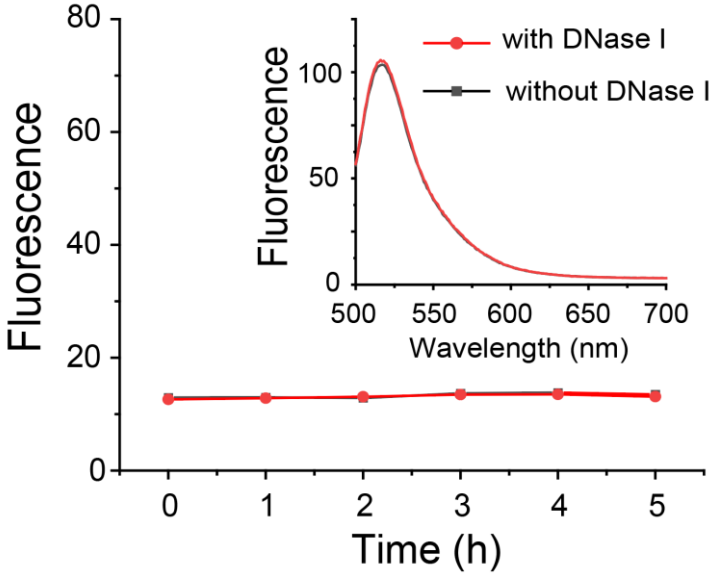

Fig. S9. The fluorescence intensities of 8 nM polyA20-SNA in buffer with (red dots) or without (black dots) 0.25 U/mL DNase I were measured as a function of time. The inset shows the fluorescence curves of polyA20-SNA (8 nM) after incubation with (red line) or without (black line) 0.25 U/mL DNase I in the presence of 100 nM miRNA-21.

Following incubation of 8 nM polyA20-SNA with or without 0.25 U/mL DNase I for various durations, it was observed that fluorescence levels remained nearly unchanged in the absence of a target, suggesting that the probe is resistant to degradation by DNase I.[3] After the target gene was added, the RNA walker was activated, leading to the recovery of fluorescence (inset). It was found that the fluorescence intensity was minimally affected by the presence of DNase I, indicating that polyA20-SNA can withstand nonspecific enzyme degradation in complex biological environments.

Table S2 Recovery assays of three kinds of miRNAs in 10-fold diluted human serum samples.

Samples	Added (nM)	Found (nM)	Recovery (%)
miRNA-21	1	0.95 ± 0.017	95
miRNA-486	1	1.02 ± 0.023	102
miRNA-155	1	1.07 ± 0.025	107

References

1. K. Jiao, Q. Yan, L. Guo, Z. Qu, S. Cao, X. Chen, Q. Li, Y. Zhu, J. Li, L. Wang, C. Fan and F. Wang, *Angew. Chem. Int. Ed.*, 2021, **60**, 14438-14445.
2. X. Qiu, H. Zhang, H. Yu, T. Jiang and Y. Luo, *Trends Biotechnol*, 2015, **33**, 180-188.
3. D. Zhu, X. Li, Y. Zhu, Q. Wei, Y. Hu, S. Su, J. Chao, L. Wang and L. Weng, *ACS Appl. Mater. Interfaces*, 2023, **15**, 15250-15259.